

# A98-31661

ICAS-98-5,10,3

## Aerodynamic Integration of High Speed Propeller on Aircraft Recent Investigations in European Wind Tunnels

Alain Dumas, Claude Castan  
Aerospatiale, Aircraft Business  
316 route de Bayonne, 31060 Toulouse, France

### 1. Abstract

Pushed by the needs of fuel burn reduction (cost effectiveness and environment quality) as well as competitive US research effort, the European industry promoted a new generation of high efficiency aircraft (15 to 25% fuel saving) driven by the advanced propeller technology. The key-unknowns were mainly the high speed aerodynamic behaviour and the noise.

In 1990, the European Commission launched a ten years cooperative programme dedicated to the integration of such transonic propeller on transport aircraft. Part of it was GEMINI II, funded in June 94 to investigate the aerodynamic interactions between a propeller slipstream and a typical commuter airframe at transonic speed (Mach 0.72). During thirty-three months Aerospatiale coordinated it in cooperation with Alenia, CASA, Dornier, Ratier-Figeac, CIRA, ONERA, University College Galway, ARA, NLR and AirTechnologies. It was divided under four main tasks aiming at the performance of a wind tunnel test in the ONERA transonic facility S1 Modane. First workpackage was to produce a model (full span, with engine simulation) on the basis of the aerolines generated by the same team under the Brite-Euram GEMINI pilot phase (1990-93) already funded by the EC and placed under Aerospatiale coordination. Second workpackage was to produce the corresponding powerplant (transonic propellers, air driven turbines, rotating balance...), third was the preparation and execution of wind tunnel test and the last was covering all computational activities needed to prepare the test, predict the phenomena and ease experimental observation.

In parallel to this fundamental effort, Aerospatiale developed a more industrial one from 1994 on : a 1/9.5 scale half model of the four-propeller Future Large Aircraft (FLA) to be tested in the same wind tunnel (S1). This was the result of a combined effort of ONERA and Aerospatiale with the financial support of SPAé. Purpose was to study engine installation effects and the slipstream influence on the aerodynamic performances of the aircraft at Mach number range from 0.6 to 0.72. The model was equipped with 2 six bladed propellers driven by the same air turbines as GEMINI II and the wing was equipped with air supply and return ducting going through the wall balance via a decoupling system. The propeller performances were obtained by using a balance installed inside the nacelle, the hub of each propeller being further equipped with a torque meter. The global aerodynamic loads on the model as well as pressure distributions on the wing, nacelles and fuselage have been measured.

### 2. Abbreviations

CT Thrust Coefficient (Propeller definition)

$$CT = \frac{F_n}{\rho \cdot N^2 D^2}$$

where  $F_n$  is the propeller net thrust (blade loads),  
 $\rho$  is the air density  
 $N$  is propeller rotation speed (run per sec)  
 $D$  is the propeller diameter

CTA Thrust Coefficient (Aircraft)

$$CTA = \frac{F_n}{Q_0 \cdot S_{ref}}$$

where  $F_n$  is the propeller net thrust  
(given for one propeller),  
 $Q_0$  is the dynamic pressure  
 $S_{ref}$  is the aircraft wing reference area

J Advance Ratio

$$J = \frac{V}{N \cdot D}$$

where  $V$  is the forward (aircraft) speed,  
 $N$  is propeller rotation speed (run per sec),  
 $D$  is the propeller diameter

### 3. GEMINI II Model

Model design and manufacturing was shared amongst partners as a real industrial programme.

#### 3.1 Fuselage

The fuselage was split under the following sub-elements:

- a nose part and an aluminum front extension ring (PSI modules, electrical inclinometers and Mass Flow Control Unit were located in the free central zone of this structure), manufactured by Aerospatiale,
- a central part and a sting interface, made out of high strength steel (110 hbars) after heat treatment to insert the balance package (balance, airbridges, sting interface) manufactured by Alenia,
- a rear part made of aluminum, manufactured by Aerospatiale.

Fuselage parts were delivered to Aerospatiale model workshop between January 96 and April 96 for final

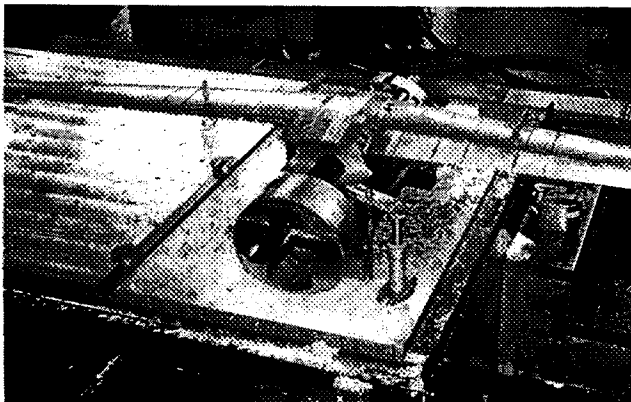
assembly. The complete fuselage was finally shipped to Modane wind tunnel in October 1996.

### 3.2 Wing

The wing consisted of two main sub-assemblies:

- the removable leading edges, designed to give access to the instrumentation installed in the nacelles, during the tests and the fixed flaps (clean configuration), designed to allow future implementation of movable flaps for high lift configurations, manufactured by Aerospatiale,
- the wing box, consisting of two outer wing parts and a single piece of high strength steel inner wing with grooves cut in the upper surface to duct pressurised air to the nacelles and closed by electron beam welding under CASA responsibility

Manufacturing of the wing box was complex and parts were delivered to the model workshop in July 96 (see picture 1) for final assembly, pressure taps installation (448 ports) and pressure tests.



Picture 1

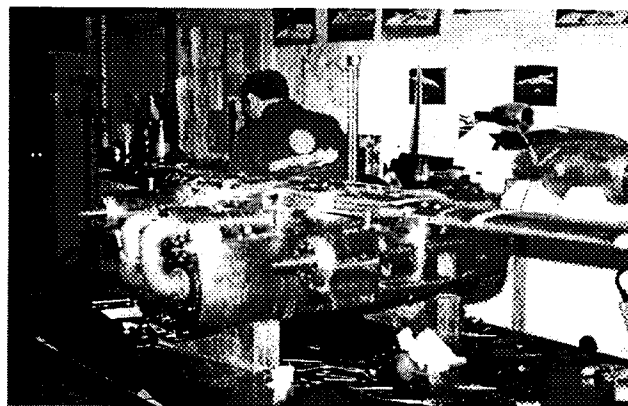
Checks performed on the wing have shown a very high quality standard. The high pressure duct sustained up to 200 bars and the low pressure duct up to 80 bars. Profile geometry was within 0.1 mm accuracy, dihedral check showed a negligible tip deviation upward of about 1.0 mm for a total span of 3.1 m. After installation on the fuselage, residual yaw angle was in the order of 0.01°.

### 3.3 Nacelles

The nacelles were designed and manufactured by Aerospatiale. They consisted of a steel central structure plus rear and front parts all made available by January 96 and instrumented with 44 pressure ports. They were pressure proven in October 96 and shipped to Modane in November 96. Their integrity was demonstrated up to 90 bars on the HP side and 30 bars on the LP side.

### 3.4 Model Final Assembly

Complete model instrumentation, assembly and commissioning were done in a central site (Aerospatiale) to ensure quality of the final product, from August to November 96. Various checks were performed after reception of the components and, to ensure a good quality of the connections, all screw holes were dug on the fuselage central part together with the wing and the other fuselage parts. Removable leading and trailing edges of the wing were assembled on the main box and pressure tapping started. The leak check was performed with the fuselage central part, wing and nacelles fully assembled to test the complete pressure circuit at once (picture 2).



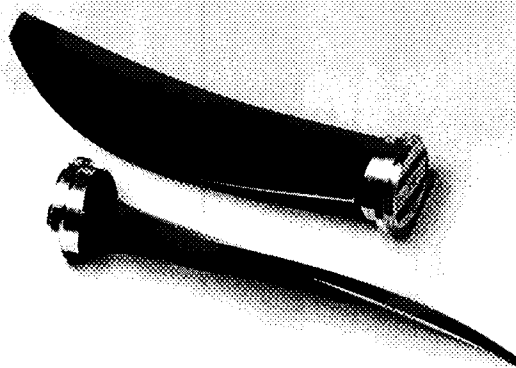
Picture 2

## 4. GEMINI II Powerplant

### 4.1 Propellers and hubs

The GEMINI II propeller, so-called SAPI, was originally designed for GEMINI pilot phase by Ratier and Hamilton for a high speed commuter (50 seats, Mach 0.7). It consists of a six-bladed prop based on NACA16 airfoils :

Scale	Parameter	Take-off Mach 0.30	Cruise Mach 0.70
Full (3.75 m)	RPM	1110	900
	Power (shp)	5384	3015
	Thrust (N)	29721	8082
	Efficiency	0.756	0.763
Model (0.469 m)	RPM	8877	7911
	Power (shp)	79	111
	Thrust (N)	436	271
	Efficiency	0.756	0.763



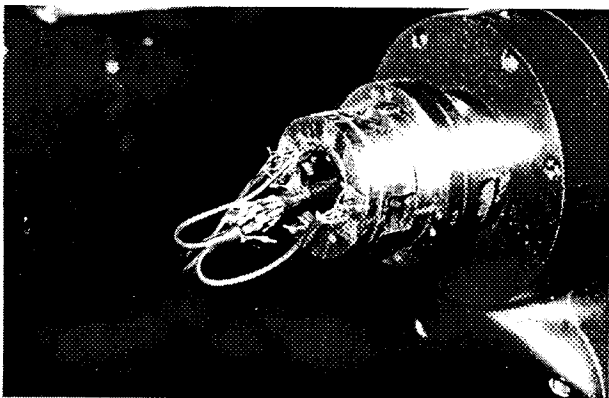
Picture 3

NLR designed and manufactured two propeller sets based on shapes and specifications provided by Ratier-Figeac. Twenty-one full carbon-epoxy blades were manufactured (see picture 3) to cover prove-out, tests and serial phases. Fourteen of them were delivered for wind tunnel tests (two spares) within two were equipped with torsion and bending strain gauges.

Two hubs, spinners and dummy spinners have been manufactured in aluminum and delivered as part of propeller assemblies. Blade structural design was validated through a set of static tests including resonance frequency measurement, tension, torsion and bending overloading and fatigue tests performed on static parts. All of them were also X-Ray controlled to ensure structure homogeneity from blade to blade.

#### 4.2 Rotating balance

ARA designed a six component balance based on the loads provided by Ratier-Figeac. It consists of two active balances welded back-to-back, both strain gauged as normal ARA custom. The eight sparks were equipped with wheatstone bridges of either 4 or 8 active gauges. Balance was also equipped with 4 temperature sensors. Measured loads were obtained by combining output signals from front and rear rows. One live balance plus one dummy were manufactured by ARA and delivered in August 95 for acceptance tests at DNW-LST. Picture 4 shows this balance installed on the real nacelle.



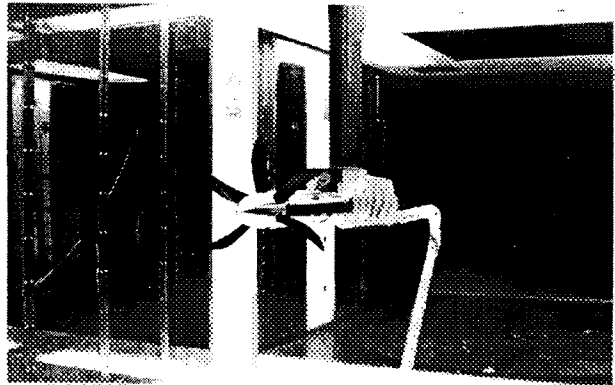
Picture 4

#### 4.3 Engine simulator

The original AirTechnologies turbines (CR21677) were upgraded for data transmission from rotating parts (blades, balance) to static parts in order to enable real time survey of blades strain gauges and rotary balance sensors by addition of Litton BN 2177 twenty-eight channel sliprings. This modification led to manufacturing of new hollow shafts to enable propeller wires to reach sliprings. Phonic wheels were used to define azimuthal reference required to determine the direction of cyclic loads measured by the balance.

Powerplant assembly behaviour was analyzed under dynamic conditions. Computations were performed by INSA Lyon (France) and AirTechnologies. They showed no critical speed problem.

#### 4.4 Acceptance Tests at LST

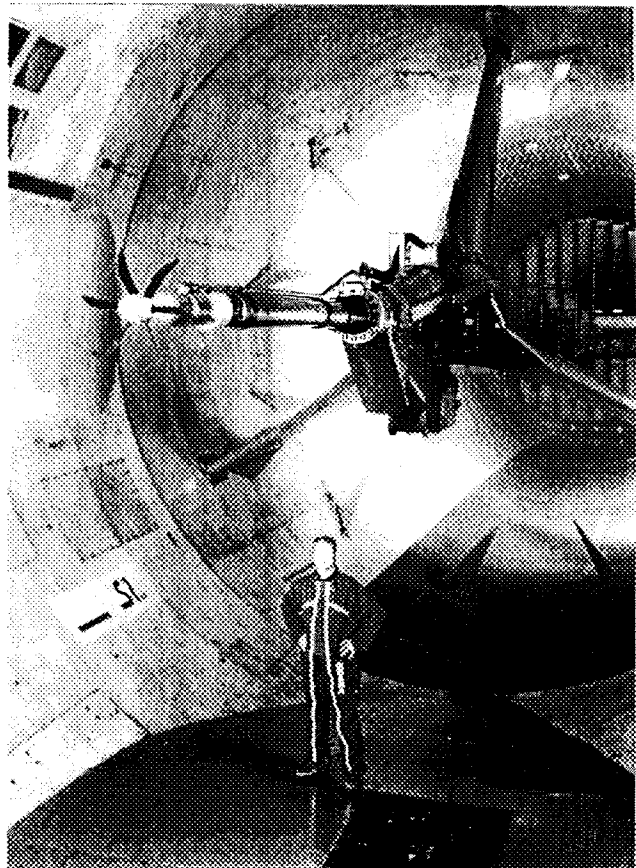


Picture 5

The acceptance test of the powerplant was performed in September 95 at NLR-LST, now DNW-LST (see picture 5). Tests were conducted by NLR and Ratier-Figeac. Configuration tested included speed up to 9400 rpm (max operational) and inflow angles up to 25°. Vibration levels, blade strain gauges and balance output were monitored and recorded. Structural integrity of the propeller and vibrational behaviour of the rotating parts have shown to be acceptable at all conditions. Propeller-to-propeller differences were negligible.

#### 5. GEMINI II Isolated Propeller Wind Tunnel Tests

##### 5.1 Test Setup



Picture 6

The isolated propeller tests were performed in cart nb 3 (45.4 m<sup>2</sup>) of S1 Modane wind tunnel, with stagnation pressure about 0.89 bars. The minimum body setup was installed on the tripod support (see picture 6, previous page). It consisted of :

- a sting holding the Technofan CR21677 turbine, the Litton slipring and in some cases a rake equipped with three five hole probes,
- an ONERA six components fixed propeller balance assembly,
- the propeller drive system, including instrumented flectors, the metric propeller shaft and the bearing assembly from ONERA,
- the dummy or live rotating balance manufactured by ARA,
- the propeller, hub and spinner manufactured by NLR.

### 5.2 Test History

Isolated propeller tests were divided under three entries in January, March and July 1996. Several concerns were identified in the rig during the first entry and the "top of climb" blade setting pre-selected (68°) was found too highly loaded, exceeding stress capabilities. The test matrix was therefore revised.

From the rig side, unbalance of the rotating parts was identified. Actually, both propellers were only statically balanced and never tested at full power. During an attempt to dynamically balance the rotating assembly it was determined that residual dynamic unbalance was of the order of 110 g.mm. The resulting centrifugal force was also responsible for ONERA balance overloading (Z, M, Y, N components). A complete dynamic re-balancing was performed, resulting in a residual unbalance of 1.7 gmm for Propeller 1 with live balance and 3.2 gmm for Propeller 2 with dummy balance.

The second entry occurred in March with properly balanced propellers. This time, the slipstream survey was successfully completed, but force measurements were questioned. The unique feature of the rig used in GEMINI II is the double balance system. Comparison between the fixed ONERA balance and the rotating ARA balance showed a perfect match for Y, Z, M and N components, but a major discrepancy was identified along X (drag). The fixed balance was reading lower thrust values than the rotating although in spite of a perfect match in wind off conditions. After analysis, two problems were found :

- the ONERA balance was affected by small movements of the turbine shaft along X axis, when in operation,
- the ARA balance was affected by the temperature rise in the tunnel, much larger than the calibrated one (up to 55°C in S1 Modane).

ONERA modified the bearing housing and flectors and instrumented them to monitor and correct if necessary parasitic loads. Then decision was made to perform a third and last entry in July to acquire data on the rotating balance for a proper recalibration. Once corrected from the thermal effects, residual discrepancy between ONERA and ARA balance was only in the order of 5 drag counts (see figure 1). Apart from the slipstream survey, valid from March, the complete test matrix was repeated successfully.

### 5.3 Analysis of Results

The unique setup used (with two independent balances in series) allows interesting data comparison and gives a very good idea of system accuracy, instead of the traditional "repeatability" analysis. Figure 1 shows the lift coefficient comparison between the fixed ONERA balance and the rotating ARA balance. The difference is well below 1% of the measured value.

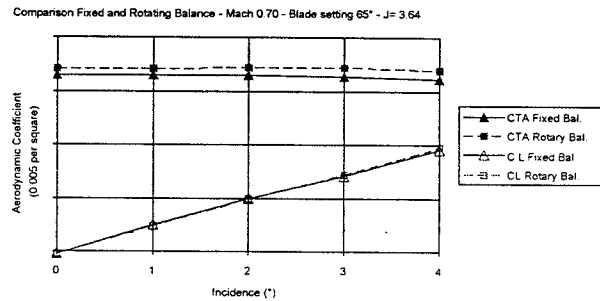


Figure 1

Also of interest is the comparison between both propellers. There, manufacturing quality is judged and NLR can be congratulated for their performance : as shown in figure 2, the difference is negligible for both thrust and lift. Same conclusion is valid for all other components. This comparison also demonstrated the accuracy of the blade pitch mechanism and set-up tool.

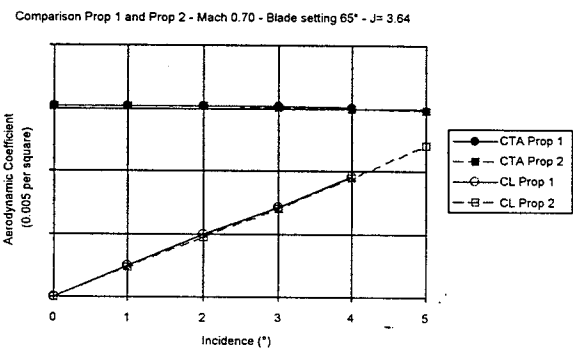


Figure 2

Propeller performance themselves are the key-results of the isolated tests. Presented here after (figure 3) are the Thrust Coefficient (Aircraft definition) and Efficiency for the three Mach numbers tested at the nominal blade setting angle (65°).

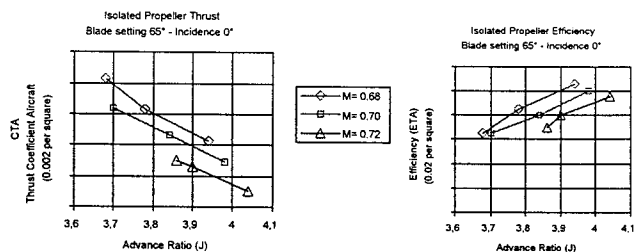


Figure 3

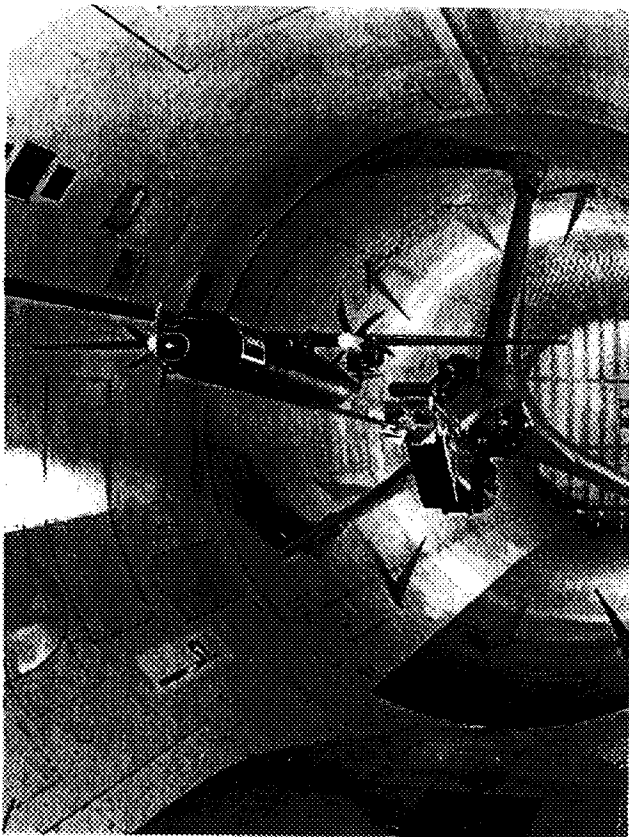
Compared with the full scale design target, this very encouraging result (experiments show performance 2 to

3% above the specification) proves the quality of Ratier-Figeac design procedure (slightly on the safe side) and the high potential of the product in powering aircraft in the transonic range.

## 6. GEMINI II Installed Propeller Wind Tunnel Tests

### 6.1 Test Setup

Setup was basically the same as for propeller isolated tests. Tests were performed in cart nb 3 (45.4 m<sup>2</sup>) of S1 Modane wind tunnel, with stagnation pressure about 0.89 bars. The full span model was installed on the tripod support, via the GEMINI hollow rear-sting and the ONERA six components balance  $\Phi$  125 nb 2 (see picture 7). The main compressed air supply (270 bars) was connected to the model to feed engine simulators.



Picture 7

### 6.2 Test History

Mid January 97, ONERA conducted flow momentum and pressure effects calibration on the complete model, fitted with dummy simulators. They consisted of main balance signal acquisition for various pressure levels in the HP circuit, in the LP circuit (both independent and without mass flow) and with various mass flow levels in the complete circuit (HP + LP).

Testing started with "props off buffet boundaries investigation". The model was shown safe as no buffet was identified up to Mach 0.72 for incidences between -3.5° and +1.5° (scheduled upper limit of GEMINI II test envelope). Tufts were installed on the model on wing upper surface and nacelle outboard side. Limitations occurred due to the model weight below predictions

(about 700 kg only), just in aero-coupling zone with tunnel fans at Mach 0.68. An option would have been to add weight in the model, but it was not possible to find any free room. Test matrix had to be restricted for the lowest Mach number where the highest incidences were not achievable within main balance load capability.

Propeller off tests with dummy simulators were completed by the end of January and the propeller dynamics were checked wind off early February. Propeller dynamics was shown very safe. Two blade settings were tested (65° and 63°) and the rotating balance was moved from port to starboard to repeat one blade setting (65°) with propeller loads measurement on the other side. By mid-February, a foreign object damaged one blade when running, luckily without any further consequence than a crater in leading edge area and a chordwise crack. Damaged blade was replaced by one spare and a short wind off run showed the balancing was perfect.

Last "props off" configuration has shown good repeatability between beginning and end of test (in the order of  $\pm 2$  drag counts), probably affected by model aging characteristics. Spinner drag was also measured with the rotating balance.

### 6.3 Data Analysis

In this paragraph, mostly forces will be discussed as Cps are analysed together with computational predictions under section 7.

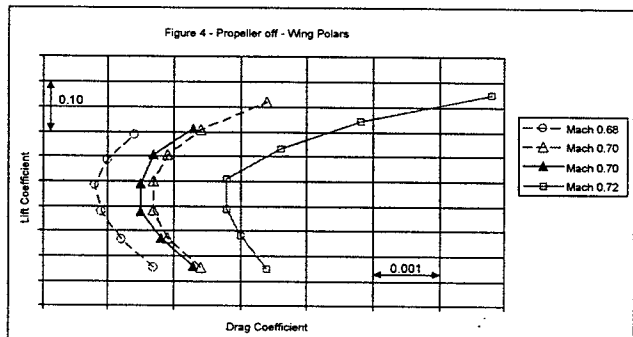


Figure 4

The initial aim was to investigate the wing buffet onset. Polars (lift versus drag) were performed for the three Mach numbers (0.68, 0.70, 0.72) as shown in figure 4. No dangerous behaviour is recorded there, although the curve is kinked at the highest angle of attack (drag rise), mostly at Mach 0.72. A repeat test at nominal Mach number gives a good idea of the accuracy (2 to 4 drag counts).

Interesting data is the propeller performance changes with installation. Figure 5 here after shows the thrust coefficient CTA as measured by the rotating balance in isolated and installed conditions for three Mach numbers. The effect is very small and Mach number dependent showing a thrust loss at Mach 0.68 and a thrust "gain" at Mach 0.72.

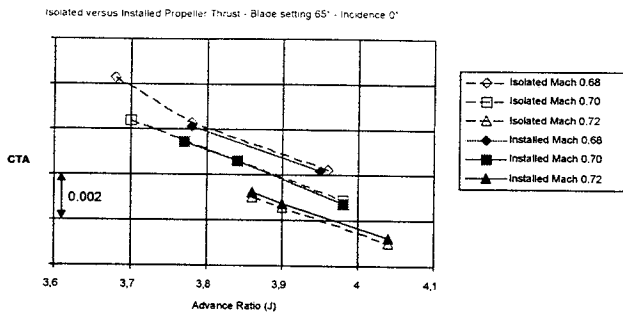


Figure 5

The key data is the slipstream effect on the airframe measured by the main balance. This means to difference between the drag measured propeller on (fully corrected from propeller forces) and the drag measured propeller off at the same lift coefficient. As shown in figure 6, drag tends to rise with angle of attack and with Mach number. For the lowest incidences appear a minimum drag.

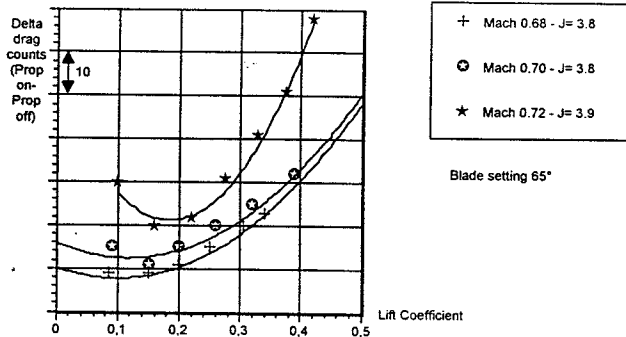


Figure 6

## 7. GEMINI II Computational Flow Field Predictions

### 7.1 Grid generation

Alenia produced the grid used by CIRA and Dornier for computation of the complete airframe configuration. A zoom on the nacelle area is shown in figure 7.

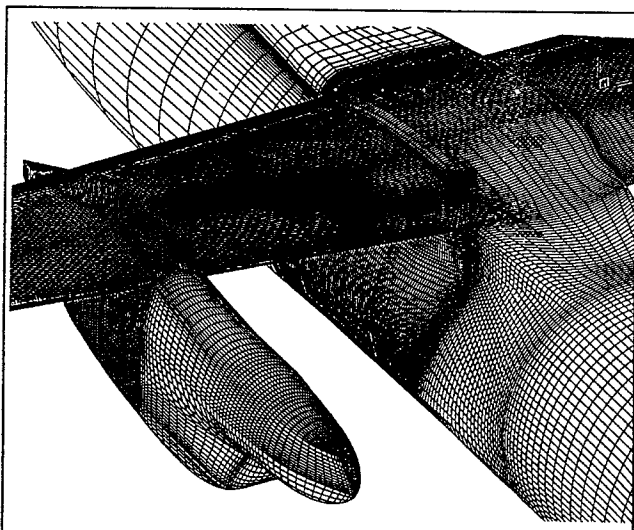


Figure 7

ONERA and UCG produced their own meshes for the propeller performance computation. The main difference between both was the spinner modelisation, completely represented in the UCG case (138 000 cells), simplified into an infinite cylindrical tube in the ONERA case. The reason for ONERA to simplify the spinner was the need to use a larger grid for implementation of the wing as a second step. They produced a 2D wing based on the airfoil in the symmetry plane of the nacelle to investigate the installation effect on the propeller. The resulting mesh (150 000 cells) was the combination of a rotating domain (the one produced for isolated propeller computation) and a fixed domain shaping the wing, as shown in the following figure 8.

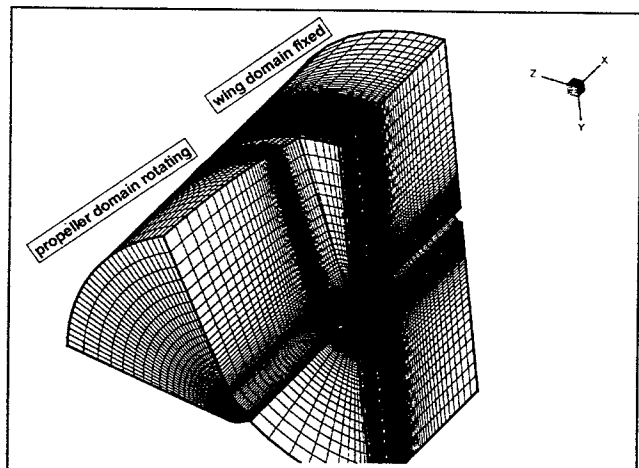


Figure 8

### 7.2 Propeller flow field prediction

The UCG solver is a 3D compressible Euler finite-volume code to predict inviscid flow around the propeller. It solves integral equations of the conservation of mass, momentum and energy. The equations fully describe the 3D dynamics of an inviscid compressible fluid and the predicted flow field variables in the domain downstream are circumferentially averaged at an axial location behind the propeller, giving the radial variation of flow field properties for the actuator disk definition.

The ONERA code (CANARI) is a 3D solver for Euler equations and for the averaged Navier-Stokes equations associated with a turbulence model. Used as well for aircraft as for turbomachinery configurations, CANARI is based on a cell-centered multi-domain finite volume approach. All types of structured grids can be mixed together with adjacent or overlapping domains.

UCG and ONERA actuator disks compare well in terms of total temperature and total pressure rise. The "installation effect" identified by ONERA is minor. As shown in figure 9, for swirl and contraction angles the situation is very different depending on wing presence: swirl and contraction angles are doubled close to propeller root (in the vicinity of the nacelle) when the wing is on.

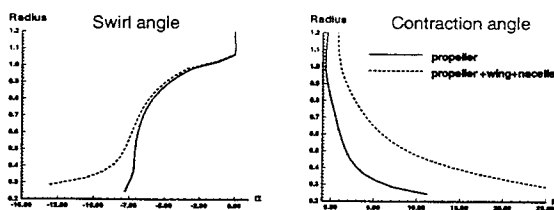


Figure 9

Isolated computations of the propeller have been performed by ONERA. For cruise conditions actuator disk data have been provided to the airframer group. Although the thrust coefficient is slightly overestimated by comparison with the S1Ma isolated propeller experiment at a fixed blade angle setting, the evolution of thrust with advance ratio is well predicted.

To investigate the mutual interference between propeller and wing a specific interface was developed by ONERA. The circumferentially averaged values of the flow field are exchanged on the interface between the upstream domain for the propeller which is rotating and the downstream domain for the wing, which is fixed. The two computational domains were shown on figure 8. As described above, the flow field characteristics are modified by the presence of the wing and the nacelle. The increments are directly related to the thrust coefficient.

### 7.3 Airframe flow field prediction

The Dornier solver is the so-called FLOWer code. It solves compressible 3D Reynolds averaged Navier-Stokes equations or Euler compressible equations, based on a finite volume formulation with multiblock structured grid. The CIRA solver (ZEN) is a multizone code solving both Euler and Reynolds Averaged Navier-Stokes equations using multiblock structured grid with capability of simulating the slipstream induced by a propeller on the aerodynamic flow field. The k-epsilon and Baldwin-Lomax turbulence model are used to close the Reynolds Averaged Navier-Stokes equations.

All computations were performed before testing (blind). A consequence was the specification at fixed incidence angle, instead of fixed lift coefficient. This tends to favour the prediction of  $C_p$  peak at the leading edge, rather than the shock position at the back.

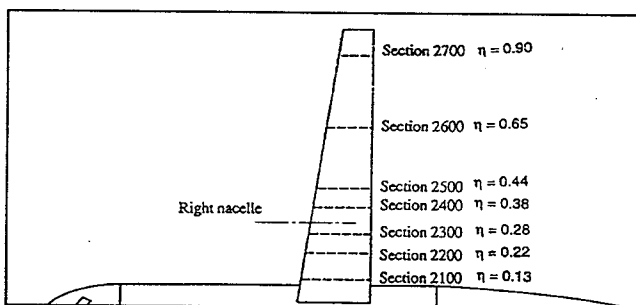


Figure 10

All computations were done on half model to save CPU time (the wind tunnel model was instrumented both sides), but with both sense of rotation simulated to represent both wings. This is acceptable for the propeller off conditions, but introduces a bias when the propeller is on : the non-symmetrical slipstream affects the flow field

around the symmetry plane. An example of wing  $C_p$  comparison between CIRA and Dornier Euler computations is shown in the figure 11, where a good agreement is visible.

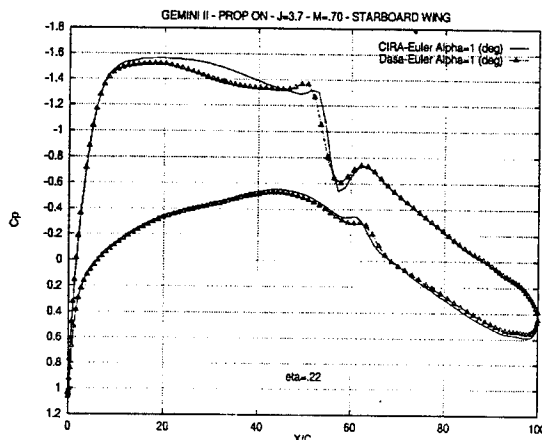


Figure 11

At Mach 0.7, incidence  $1^\circ$ , with propeller off, some small discrepancies appeared on the upper surface for the peaks and the shock definition, Dornier results containing a higher amount of artificial dissipation. Propeller on, a good agreement is found on  $C_p$ s of both wings. Differences are similar to those identified for the propeller off case. In addition, minor discrepancies in the actuator disk model are visible in the wing sections downwashed by the propeller slipstream.

### 7.4 GEMINI II - CFD versus Wind Tunnel Data

#### 7.4.1 Isolated Propeller Performance

UCG performed an analysis to compare S1Ma data to post-test-computations. First is the comparison between the UCG predicted slipstream and the measurement performed with the five hole probes rake installed on the minimum body. The signals of the five hole probes were processed to provide time-averaged measurement of the velocity components and total pressure. For comparison, the CFD calculations were circumferentially averaged to give equivalent information. The measured and predicted data are in very good agreement. Example is shown in figure 12 (relative tangential velocity).

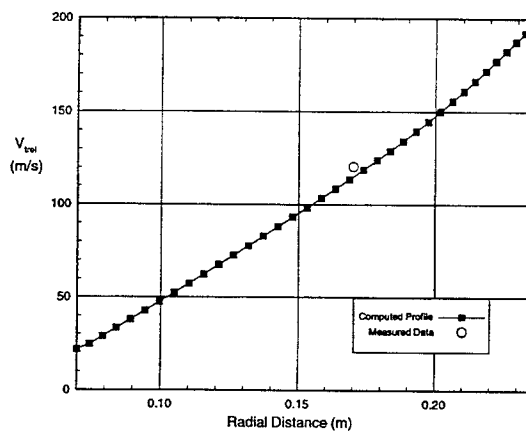


Figure 12

Concerning forces, the computed thrust coefficients of both ONERA (pre-test) and UCG (post-test) are slightly overpredicted as shown in figure 13, but they follow the measured gradient.

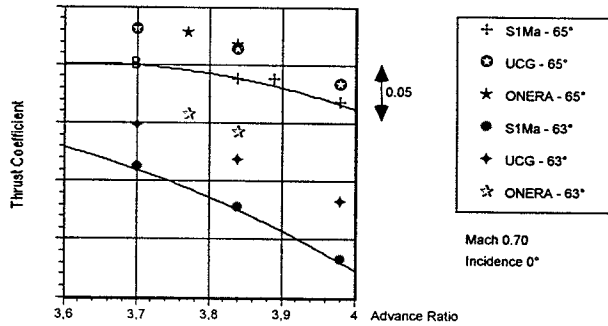


Figure 13

### 7.4.2 Effect of wing on propeller

In figure 14, the comparison of pre-test computed thrust coefficient with experiment shows that installation effects are well predicted (thrust increase). For the advance ratio computed ( $J = 3.77$ ), the ONERA code predicted a DCT of +0.036 as the experimental interpolated value is in the order of +0.040. Having seen the assumptions made in the geometry (2D) this accuracy is regarded as a success.

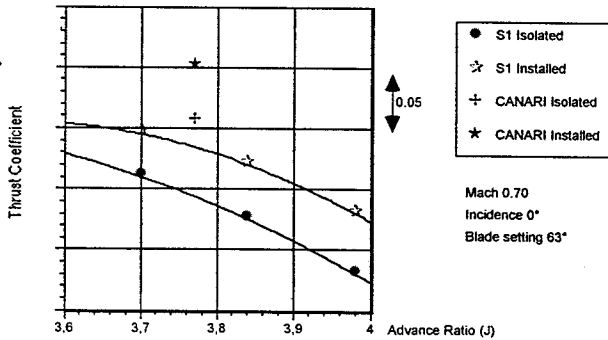


Figure 14

### 7.4.3 Complete Airframe

Figure 15, compares computations performed by Dornier and CIRA to the experiment in S1. Both the computed and the measured lift are corrected from propeller effects. As expected, we can see that discrepancies are found in the lift coefficient. For power off condition, the numerical "lift versus incidence" slope is somewhat higher than the experimental one. At zero incidence, computed lift is higher than measured one. Lift differences due to Mach number appear well predicted.

Comparing the power on and power off experimental lift, it appears that the CT effect is a small increase of the zero lift incidence, while the slope does not change. The prediction introduced an approximation due to the slipstream effect problem in the symmetry plane. Global CL was computed by simple addition of predicted port and starboard figures. The trend of lift decrease when comparing propeller on with propeller off (so-called CT effect) is clear from the test data, but not from the computation.

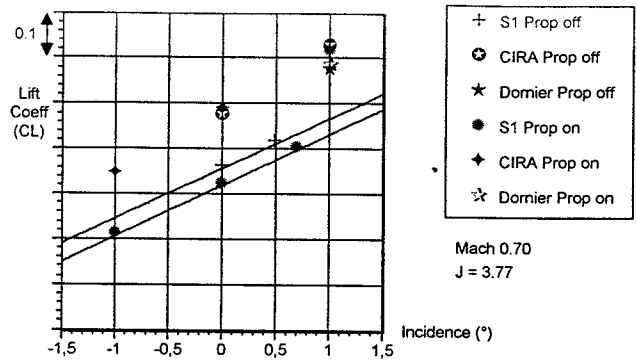


Figure 15

Looking at wing pressure distribution, the comparison of prediction and measurement is rather satisfactory, keeping in mind that CL was not fitted in the calculations.

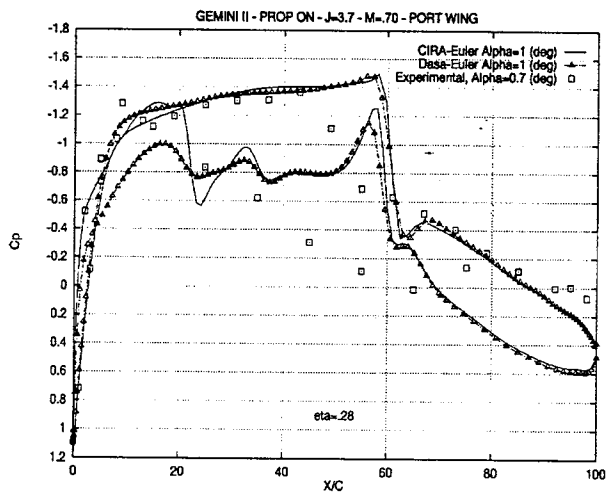
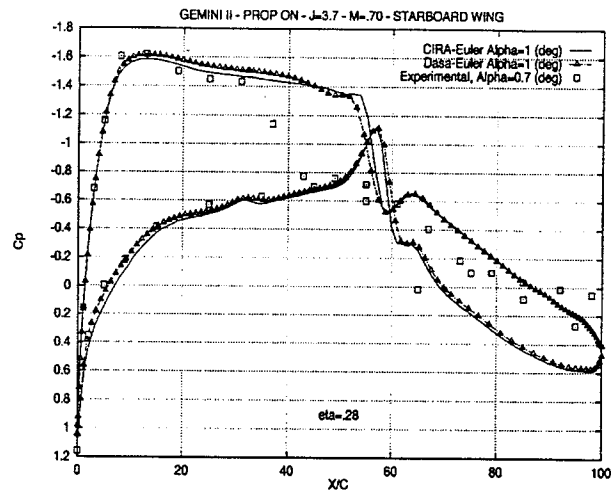


Figure 16

Four remarks are important:

- the peaks of pressure coefficient are in good agreement. Euler solver might overestimate the super-velocity at the leading edges. This was reduced by some spurious entropy production introduced at the leading edges of the wing, as a consequence of the H topology.

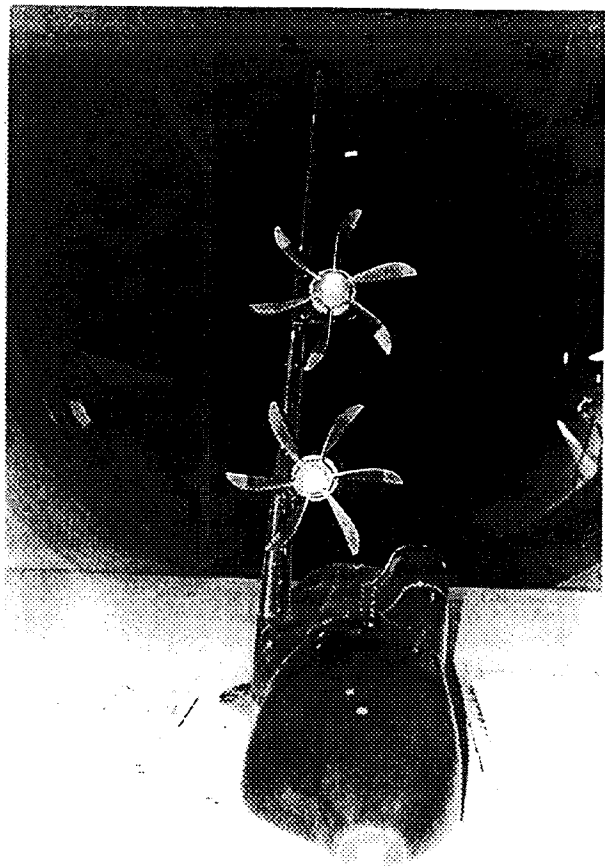


- the numerical rear pressure recovery is higher than the experimental one, due to the inviscid model and to Reynolds number effect in S1 (3 millions about). The computational solution in the rear part of the section is "rotated" downward and the rear loading higher than the experiment.
- separations were identified in the vicinity of the nacelle during testing. In the Euler simulation a supersonic area is found near the rear part of the nacelle to wing intersection. This leads to a meaningful difference between numerical and experimental data on the lower surface of the wing (see figure 16).
- the predicted shock is stronger and located more downstream than the experimental one, due to the inviscid model used for computations and to the fact that comparison is made at a given angle of attack. Nevertheless, slipstream effect (that tends to increase the shock) is well simulated by the actuator disk model. Looking at the pressure variation induced by the propeller in the leading edge area close to the nacelles upwash and downwash on the wing are correctly represented (see figure 16).

From both experimental and numerical data it appears that propeller slipstream affects the wing pressure distribution from the vertical symmetry plane until about 60% of the span, although propeller disk extends from 18% to 45% only. The Euler simulation was indicating an increase of 1% of the lift for the starboard wing and a decrease of 3% for the port, leading to a global decrease of 2%. Spanwise pressure distributions (experimental and predicted) show that this trend is dictated by the phenomena happening on the inboard part of the wing. Starboard, the propeller induces upwash and a total pressure increase on the inboard, leading to a supersonic velocity and a decrease of static pressure on the upper surface, an increase of static pressure on the lower surface (lift increase). Port, the propeller induces downwash and an increase of total pressure on the inboard part of the wing, creating a static pressure increase on the upper surface, a supersonic velocity and a static pressure decrease on the lower surface (lift decrease). We might conclude that the CT effect on the global lift is related to a strong interference between the nacelle, the wing and the fuselage, magnified by flow compressibility.

### 8. FLA Model Description

The semi-span model manufactured by Aerospatiale was representative of the FLA aircraft with 173 m<sup>2</sup> wing area and four turboprop fitted with 6-bladed 16 feet Ratier-Hamilton propellers (see picture 8) at scale 1/9.5. Considered cruise speed was from Mach 0.60 to Mach 0.72. Model half span was in the order of 2.2 m, sweep angle 15° and aerodynamic mean chord 0.49 m and structural capability for test at 2.5 bars stagnation pressure in Le Fauga F1.



Picture 8

The propeller, designed by Ratier-Figeac and Hamilton Standard were made out of titanium and jointly manufactured by ONERA-IMFL and Aerospatiale. Their characteristics are summarized in the following table.

Propeller	Full Scale	Model Scale
Diameter (m)	4.88 m	0.51 m
Blade number	6	6
Hub-to-tip ratio	0.2	0.23
Cruise conditions	Mach 0.68 @ 31000 feet ISA	Mach 0.68 @ Ti 325 K Pi 0.9 b
Power (SHP)	7500	220
RPM	745	8300
Traction (N)	20000	500
$C_{ta} = T / (qoS) (10^{-3})$	500	500
$Re (10^6)$	~6	~1

The pitch change mechanism designed by ONERA-IMFL was using a pre-setting concept (fingers) to allow the highest repeatability.

Three nacelles were designed, one internal, one external and one "calibration" (see explanations under section 9). None of them had air inlet simulation and turbine drive air was ducted back through the wing (i.e. no exhaust either) as for the GEMINI II model (see figure 17). These nacelles were also using the same engine simulator (CR21677) as described under section 4.

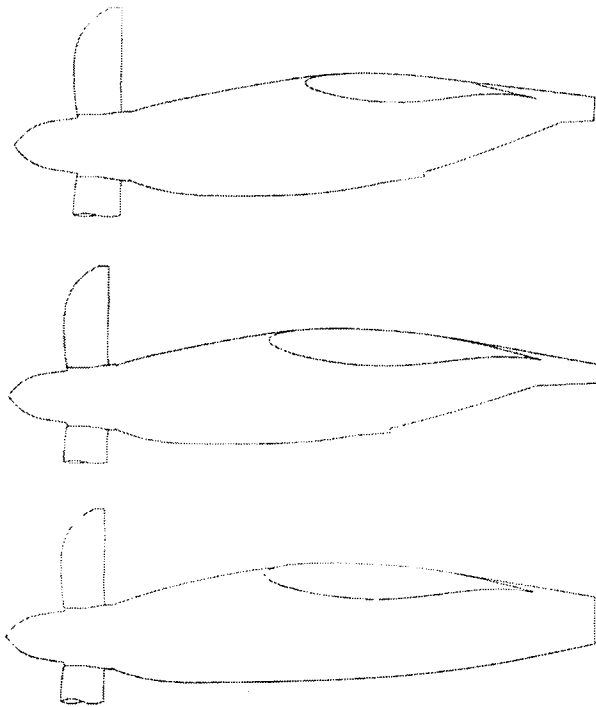
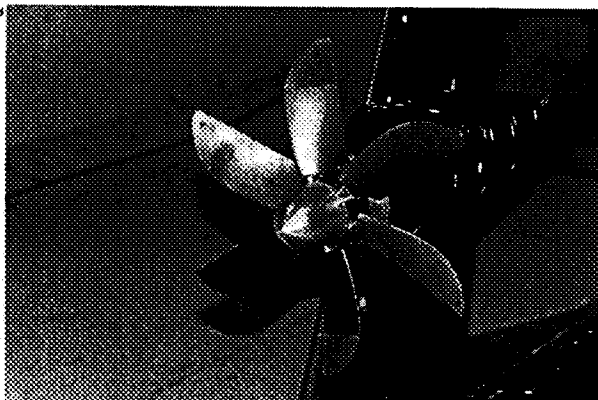


Figure 17

Picture 9 shows a closer view of one of these models.



Picture 9

Eleven rows of static pressure taps were implemented on the wing, two on each nacelle, plus some on the fuselage (450 total). In addition, accelerometers in the nacelles and strain gauges at wing root and on propeller blades were used to monitor the dynamic behaviour of the model.

### 9. FLA Test Objectives and Methodology

Test objectives were to validate testing techniques and aerodynamic design tools through the identification of wing-powerplant interaction drag at transonic speed. As a contrary to what was done in the GEMINI II programme, the methodology selected here deliberately left out the rotating balance technology. The half-model was installed on a six components underfloor balance and the calibration nacelle was fitted with a "five plus one" component balance coupled to a torque meter. Test was performed in four step :

- blade off run, with the actual nacelle to measure the airframe drag,

$$CD_1 = CD_{airframe} + 2 CD_{spinner}$$

- blade on run, with the actual nacelles and main balance measurement only

$$CD_2 = CD_{airframe} + 2 CD_{spinner} + 2TC_{props} + ACD_{airframe} + 2ATC_{props}$$

Where TC is the propeller traction as measured on the minimum body, ACD is the slipstream effect on the wing and ATC is the effect of the airframe on traction.

- blade on run, using the calibration nacelle to access both the main balance and the propeller static balance

$$CD_3 = CD_{spinner} + TC_{props} + DTC_{propse}$$

- blade off run, using the calibration nacelle to get both main and spinner-hub balance readings.

$$CD_4 = CD_{spinner}$$

Combination of the four gives the slipstream effect:

$$ACD = CD_2 - CD_1 - 2CD_3 + 2CD_4$$

The main underfloor balance was connected to high pressure (150 bars) and low pressure (20 bars) air bellows to uncouple parasitic loads from the drive air going to and from the engine simulators. The propeller and spinner loads were measured by the so-called "five plus one" annular static balance (five components, coupled to a high accuracy thrust dynamometer), located between the hub and the turbine crossed by the drive shaft.

### 10. FLA Test and Results

Repeatability within a run has achieved  $\pm 1.10^{-4}$  for drag coefficient and  $\pm 1.10^{-2}$  for incidence (at a given CL). The long term repeatability (two polars compared between the beginning and the end of the test campaign) have reached for power on configuration the level of  $\pm 1.7.10^{-4}$  for drag coefficient and  $\pm 2.10^{-6}$  for incidence (at a given CL).

A Mach 0.68 result is shown in figure 18. Three drag polars are plotted: wing alone, wing and nacelle power off and power on case. A logical increase of the drag is shown, due to the installation of the nacelle and the disturbance from the slipstream.

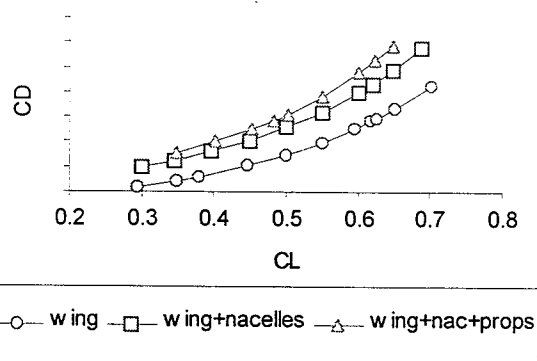


Figure 18

Looking deeper at these disturbances, figure 19 compares lift distribution versus span for the same cases (positions of the inboard and outboard engine are indicated). The lift drop is clear, especially behind the nacelles.

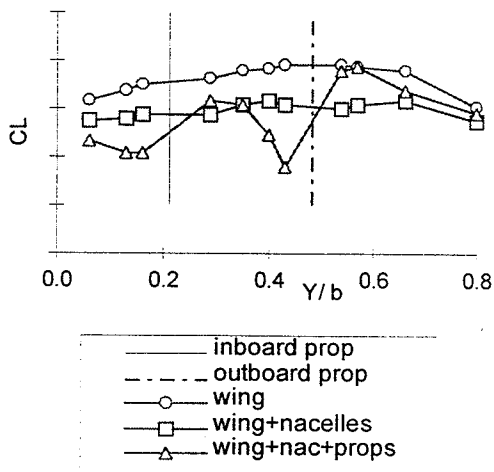


Figure 19

The slipstream effect is made of the combination of total pressure increase, flow acceleration and local incidence change. This generates a local lift and incidence increase on the upwash side and a local lift and incidence decrease on the downwash side.

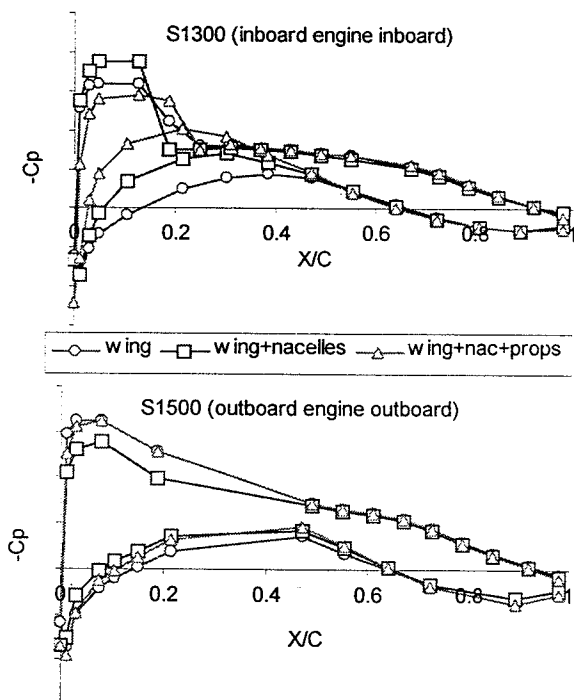


Figure 20

Looking at the pressure distribution on both side of the nacelle (e.g. the inboard one on figure 20) at Mach 0.68 and 3° incidence, one can see that:

- on the inner side of the inboard nacelle, in power off conditions already, a large overspeed is generated next to the leading edge, as well as an acceleration on the lower surface (venturi effect between the fuselage and the nacelle)
- the slipstream effect (power on) significantly reduces the lift on the inner side of the inboard nacelle (downwash effect), but the slipstream effect is to some extent compensated by the upwash on the outer side.

Same trends have been identified on the outboard nacelle.

## 11. Conclusion

Over the last decade, the "60 to 100 seats" civil market as well as the military airlift were split 50/50 between the turboprops and the turbofans. In spite of higher cost and pollution, recent forecast predicts that turbofans are taking up to 70% due to better passenger and crew comfort (i.e., noise and speed). This was not obvious by the time the EC research programme (GEMINI) was launched, as the push still was from the economics and environmentalists to introduce into service propeller driven aircraft. In-between fuel price drop has helped re-energizing the turbofan. With a cruise speed as the one achieved by GEMINI II and the FLA (Mach 0.72) the performance gap is closed and the turboprop benefits in terms of cost and pollution could be exploited again.

The noise issue is the next challenge for the GEMINI II partners. In parallel with this programme, they worked out the isolated propeller noise with another EC-funded programme called SNAAP. Purpose was to identify and predict the noise source. An enlarged team has joined forces in July 96 to initiate from SNAAP and GEMINI II lessons another EU-funded project named APIAN. This time, they are investigating the acoustics of the propeller with the airframe to define the noise on fuselage skin (at transonic speed) and the noise pattern on ground (at low speed). The full span powered model from GEMINI II will be the basic tool for this research that will end with this century, concluding a steady ten years effort.

## 12. References

- The European Programme GEMINI*, C. Castan, B. de la Puerta  
International Forum on Turbine Powered Simulation, 16-17/5/95, Emmeloord NL
- European Research Cooperation on Propellers Noise and Aerodynamics*, C. Castan, A. Dumas, P. Cloarec  
Workshop on Aspects of Airframe-Engine Integration, 6-7/3/96, Braunschweig D
- A Numerical-Experimental Investigation on Propulsion Airframe Interaction for Propeller Driven Aircraft*, M. Amato, P. Catalano  
AIDAA Congress, Naples, October 1997
- Essai d'une demi-maquette motorisée de l'avion de transport militaire FLA*, J.F. Séchaud, A. Dumas  
AAAF Congress, Marseilles, March 1998